

# Nano-Particle Deposition in Axisymmetric Annular Pipes with Thread

Pouyan Talebizadehsardari<sup>1,2,\*</sup>, Hassan Rahimzadeh<sup>3</sup>, Goodarz Ahmadi<sup>4</sup>, Mohammad A. Moghimi<sup>5</sup>, Kiao Inthavong<sup>6</sup>, Mehdi Esapour<sup>7</sup>

<sup>1</sup>Department for Management of Science and Technology Development, Ton Duc Thang University, Ho Chi Minh City, Vietnam

<sup>2</sup>Faculty of Applied Sciences, Ton Duc Thang University, Ho Chi Minh City, Vietnam

<sup>3</sup>Department of Mechanical Engineering, Amirkabir University of Technology, Tehran, Iran.

<sup>4</sup>Department of Mechanical and Aeronautical Engineering, Clarkson University, NY, USA.

<sup>5</sup>Department of Mechanical and Aeronautical Engineering, University of Pretoria, South Africa.

<sup>6</sup>School of Aerospace, Mechanical and Manufacturing Engineering, RMIT University, Australia

<sup>7</sup>School of Mechanical Engineering, Mazandaran University of Science and Technology, Babol, Iran

## Abstract

The transport and deposition of nano-particles in annular threaded pipes under laminar flow conditions was studied compared with smooth annular pipes. A 2-D axisymmetric model was used for fluid flow simulation and the Lagrangian particle tracking method was used for particle simulating. The effects of thread size and nano-particle diameters in the range of 5 to 200 nm were

---

\*Corresponding author.

E-mail address: ptsardari@tdtu.edu.vn (Pouyan Talebizadehsardari).

studied for different annular pipe lengths. For the smooth annular pipe, the Brownian excitation is the dominant force for particle deposition in the range of nanoparticles without any external force. The simulation results showed enhancement of particle deposition for pipes with threads especially for larger particles due to their inertia effects. However, for particles smaller than 40nm, the addition of threads had little influence on increasing the deposition efficiency. The maximum increase in the particle deposition was found for a thread length of 3mm where the hydraulic diameter and height of the threads are equal to 1mm. The increase was 5.3% and 33.9% for 10nm and 100nm particles, respectively, compared with a smooth annular pipe with the same length. For deposition of large size nanoparticles, the study also showed that the effect of thread decreases as the annular pipe length increases.

**Keywords:** Nano-particle Deposition; Lagrangian particle tracking method; Threaded geometry; Annular pipe; Axisymmetric model.

## **1. Introduction**

Developing new effective methods for trapping emitted particulate matters from engines have attracted the attention of many researchers (Kittelson 1998; Wichmann 2007; Kennedy 2007; Lin et al. 2015) due to its importance on human health. In particular, the negative health consequences of nano-particles are being more recognized. It is now well-known that diesel engines emit significant amounts of nano-particles in the size range of 5 to 500 nm (Talebizadeh et al. 2014; Paul et al. 2013). Petrol and compressed natural gas engines also emit significant amount of nano-particles as well as diesel engines (Ristovski et al. 2004). However, due to the higher amount of nano-particles emitted from diesel engines, more concerns are attended to them compared to petrol

engines. Furthermore, in the past, after treatment devices are focused and developed based on the mass emission standards. However, it is reported that the number and diameters of the emitted particles should also be considered (Kwak et al. 2014; Jayaratne et al. 2008; Xinling and Zhen 2009). Therefore, after Euro 5a standard in Euro 5b and Euro 6 (2011 and 2014), the permissible number of particles emitted from diesel passenger cars was added to the Euro standard, being  $6 \times 10^{11}/\text{km}$  (Johnson 2009).

Transport and deposition of nano-particles in different configurations for various applications have been studied (Lin, Lin, and Chen 2009; Wang et al. 2009; Lin et al. 2014; Tian et al. 2017; Chaumeil and Crapper 2014; Sardari et al. 2018). In particular, using Eulerian and Lagrangian approaches, nano-particle deposition in tubular pipe flows was investigated extensively (Longest and Xi 2007; Chen, Simon, and Lai 2006). The original model for the Brownian motion of nano-particles in Lagrangian simulations was introduced by Li and Ahmadi (1993) and Ounis et al. (1993). Earlier, Eulerian diffusion-based theoretical models and empirical expressions for particle deposition in smooth tubes were developed (Thomas 1967; Ingham 1975, 1991; Yeh and Schum 1980; Cohen and Asgharian 1990; Martonen, Zhang, and Yang 1996). In addition, the Eulerian-Lagrangian particle tracking method was used for evaluating the deposition of nano-particles in respiratory passages and nasal cavity in the literature (Zamankhan et al. 2006; Inthavong, Zhang, and Tu 2009; Ge, Inthavong, and Tu 2012). In these studies, the simulation results were verified by comparing the predicted nano-particle deposition efficiency with the empirical equations for duct flows.

In contrast to the rather large number of studies on tubular pipe flows, the Brownian diffusion of nano-particles in annular pipes has hardly been reported in the literature. Annuli with circular or rectangular cross-sections have many industrial applications including heat exchangers and

electrostatic precipitators. Chang et al. (1995) studied experimentally and numerically the effects of Brownian diffusion and thermophoresis on the deposition of glass aerosols in annular flows with thermal gradients between two cylinders. Using experimental and computational approaches, Tsai et al. (2004) investigated the deposition of nano-particles in the range of 38 to 500 nm in a tube considering electrostatic, thermophoretic and Brownian diffusion. Talebizadeh et al. (2016a) performed Lagrangian particle tracking simulations and analyzed the dispersion and deposition of nano-particles in tubular and annular pipes with application to dielectric barrier discharge reactors. A time history analysis of particle deposition was performed aims to achieve a higher particle removal.

An effective method for increasing the particles deposition rate, as well as, the particle residence time in a passage, is adding threads or baffles in the flow passage (Talebizadeh et al. 2015). While the influence of adding threads on particle deposition is well known, a quantitative analysis of the enhancement of capture efficiency has not been fully reported in the literature. Goula et al. (2008) performed a CFD simulation on the effect of a feed flow control baffle on the efficiency of sedimentation tanks in potable water treatment. Their results showed the presence of baffle significantly improves the sedimentation rate.

In this study, the effect of adding threads in annular pipes on enhancement of nano-particle deposition efficiency was analyzed. The threads were added to the inner cylinder and act as sequence of obstacle in the flow direction. The Lagrangian particle tracking method was used and the deposition efficiencies of nano-particles in annular pipes with and without threads under the laminar flow condition were evaluated for different pipe lengths. An axisymmetric computational model was used and the deposition efficiencies for different thread geometries for a range of particle sizes were calculated. Validation of the computational model was performed for the fluid

and particle flows in smooth annular pipes in the absence of treads. The results of this paper could find applications in the use of thread for enhancing particle removal efficiency in gas-particle separation devices.

## **2. Mathematical modelling and methodology**

### *2.1. Fluid Flow modelling*

For incompressible, steady and laminar airflow, the governing equations are the well-established conservations of mass and momentum. For the numerical solution, the discretized forms of these equations including the Navier-Stokes equation are obtained by integrating over the control volume. An axisymmetric model was used, due to the geometry of the duct and since there is not circumferential gradient in the flow ("ANSYS Fluent Theory Guide, ANSYS, Inc." 2018). A constant inlet velocity of 3.86m/s is used at the inlet, which is equivalent to a flow rate of 8 l/min. The outer and inner diameters of the annular pipe is 6 mm and 5 mm, respectively, and two different lengths of 40 cm 60 cm are also considered. The density and viscosity of the air are 1.225 kg/m<sup>3</sup> and 1.84E-05 kg/m·s, respectively. The Reynolds number based on the flow velocity and the annulus gap of 1mm is 257 in this study. It is noteworthy that the selected value for the flow rate is lower than those of the diesel engines flow rate. The employed condition is suitable for after treatment systems such as dielectric barrier discharge reactors and separation devices which need higher residence time for the flow and therefore operate at lower fluid velocity (Talebizadeh et al. 2016b). As mentioned, due to higher amount of nanoparticles produced by diesel engines, the results of this study could also provide guidelines more for diesel engine application rather than petrol engines. However, the flow of the exhaust gas form diesel engines is typically in turbulent flow region if the after treatment system is directly placed after the engine.

## 2.2. Lagrangian particle equation of motion

A one-way coupled assumption was used and the trajectories of mono-disperse submicron particles ranging from 5 nm to 200 nm were modelled using the Lagrangian trajectory analysis (Abouali and Ahmadi 2005). Due to the nano-particle size range used in this study, the Brownian excitation is the dominant force for particle dispersion and deposition. Other forces such as gravity and Saffman lift forces were not considered as they are negligibly small (Talebizadeh et al. 2016b). Therefore, the appropriate equation for spherical particle motion can be expressed as (Li and Ahmadi 1992b; He and Ahmadi 1999):

$$\frac{du_i^p}{dt} = \frac{18\mu}{d_p^2 \rho_p C_c} (u_i^s - u_i^p) + F_{Brownian} \quad (1)$$

where  $u_i^p$  and  $u_i^s$  are, respectively, the components of the particle and local fluid velocity,  $\mu$  is the fluid viscosity, and  $\rho_p$  is the particle density. Here  $C_c$  is the Cunningham correction factor to the Stokes drag law and is given as (Li and Ahmadi 1992a):

$$C_c = 1 + \frac{2\lambda}{d_p} (1.257 + 0.4e^{-1.1d_p/2\lambda}) \quad (2)$$

where  $\lambda$  is the mean free path of air which is equal to 65 nm under normal conditions.

The Brownian excitation is modeled as a white noise process. In the simulations, the amplitude of the Brownian force is given as (Ounis, Ahmadi, and McLaughlin 1993),

$$F_{Brownian} = \zeta \sqrt{\frac{\pi S_0}{\Delta t}} \quad (3)$$

where  $\zeta$  is a zero-mean, unit-variance independent Gaussian random number,  $\Delta t$  is the time-step used for integration of particle equation of motion, and  $S_0$  is the spectral intensity of Brownian excitation given as,

$$S_0 = \frac{216\nu k_B T}{\pi^2 \rho_g d_p^5 \left(\frac{\rho_p}{\rho_g}\right)^2 C_c} \quad (4)$$

In the above equation,  $T$  is the absolute temperature of the fluid,  $\nu$  is the kinematic viscosity,  $k_B$  is the Boltzmann constant and  $\rho_g$  is the gas density.

### 3. Geometry, boundary condition and material

Adding the baffles inside a passage is expected to increase the particle deposition rate, as well as, the gas and particle residence times. The effect of baffles on the gas residence time in the annulus was studied by (Talebizadeh et al. 2015), in this study the effect of threads on particle deposition efficiency is investigated. In contrast to the usual usage of threads that are placed as obstacles in the flow direction, the threads in this study is carved into the pipe walls along the flow direction, which has not been studied in the literature. This helps making sharp points in the domain which is useful in some applications such as non-thermal plasma in dielectric barrier discharge reactors results in a higher electrical discharge intensities. Moreover, the studied threads helps to prevent reducing the flow rate and enhancement of pressure drop. Three different thread configurations in the annulus behaving as baffles inside the annulus passage were examined. The thread height was fixed at 1 mm and the gap between threads, and thread lengths were varied in these simulations. The gap sizes used were 1, 2 and 3mm, while the thread lengths were equal to the gap between the threads in all cases.

Figure 1 shows a schematic of the sectioned of axisymmetric annular pipe with the different geometric parameters. Here “a” and “b” are the height and the length of the thread, respectively, and “t” is the distance between two consecutive threads. The height, “a” is fixed at 1 mm, and “b” and “t” are assume to be equal, being set to 1, 2 and 3 mm. The total annulus length was 400mm

and the threaded region length was 200mm. In this study, the particles were injected at the inlet surface 100mm upstream from the first the thread.

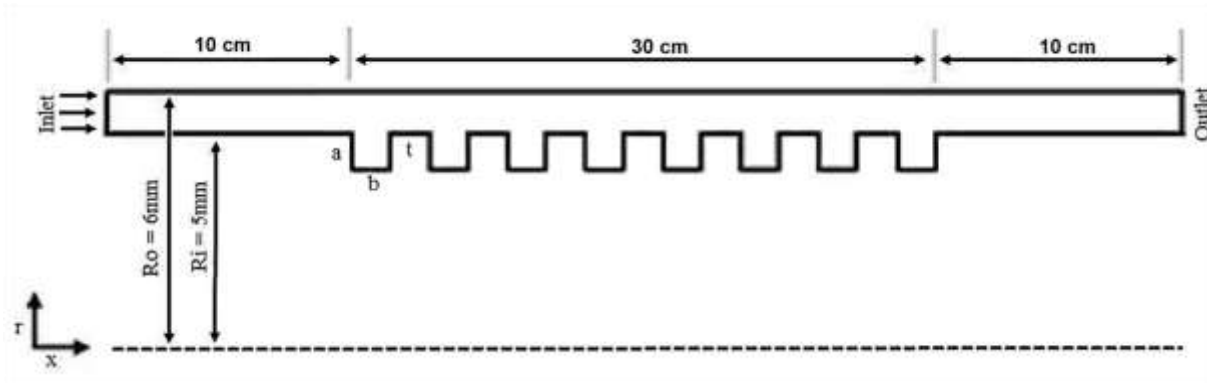


Figure 1. A schematic view of the annular pipe with threads.

Carbon was considered as the particle material which has a particle to air density ratio of 2000. The commercial ANSYS-Fluent software is used for solving the governing equations using the second-order upwind scheme for the continuity and momentum equations.

A constant velocity was imposed at the inlet boundary. For a gap size of 1mm, it is found that after a short distance about 5 cm from the inlet, the flow reached a fully developed condition. Therefore, to study the deposition efficiency in a fully-developed flow, the deposition efficiency is calculated after  $x=5\text{cm}$ , where the flow was fully developed and the analysis ended at  $x = 40\text{cm}$ . The outflow boundary condition was set at the outlet and a no-slip condition at the wall. It also is assumed that when a particle reaches a wall, it will stick to it with no rebound due to the van der Waals force which is quite large for the size of the nanoparticles. The computational grid contained uniform quad mapped mesh elements with different numbers of nodes in the x and y direction generated using the ICEM CFD code. The total number of grids for the smooth and threaded pipes were, respectively, 120,000 and 150,000. It should be noted that different numbers of particles are tested



to make sure that the results are independent of the number of particles used. Figure 3 shows the variation of particle deposition efficiency (DE) in terms of number of injected 20nm particles. The deposition efficiency is defined as the ratio of number of deposited particles to the number of injected particles. Figure 3 shows that the value of DE for different number of particles approaches an asymptote as the number of particle increases to 20,000; however, in order to increase the accuracy of the results, 60, injected particles were used in these smulations.

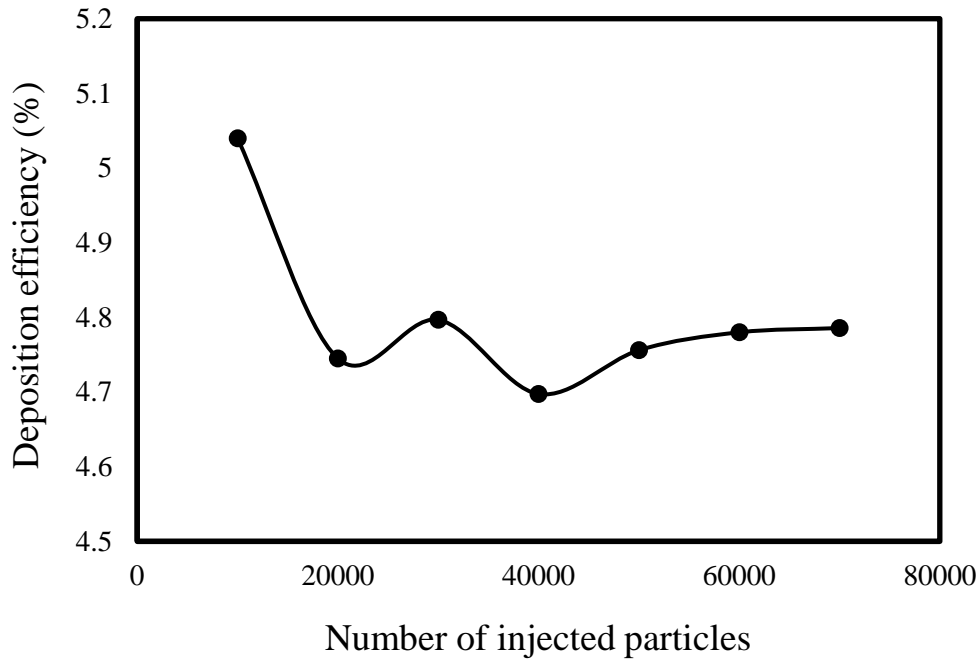


Figure 2. The variation of deposition efficiency in terms of number of injected particles.

## 4. Results and discussion

### 4.1. Validation

To verify the flow field of the axisymmetric model, the predicted velocity profile for the smooth annular pipe is compared with the exact solution. The velocity profile for a fully developed laminar annular flow is given as (Lamb and Caflisch 1993):

$$u(r) = \frac{2U_a [r_2^2 - r^2 - 2r_m^2 \ln(r_2/r)]}{r_2^2 - r_1^2 - 2r_m^2} \quad (5)$$

where

$$r_m = \sqrt{\frac{r_2^2 - r_1^2}{2 \ln(r_2/r_1)}} \quad (6)$$

In the above equations,  $r_2$  and  $r_1$  are, respectively, the outer and inner radius of the annular pipe.

Figure 3 compares the predicted fully developed velocity profiles at different locations in the smooth annular pipe with Eq. (5). The predicted velocity profiles show excellent agreement with the analytical solution verifying the present computational model. Furthermore, the velocity profiles at different locations are displayed show that the flow reaches to the fully developed condition in the annular pipe at the distance of  $x = 5\text{cm}$  from the inlet.

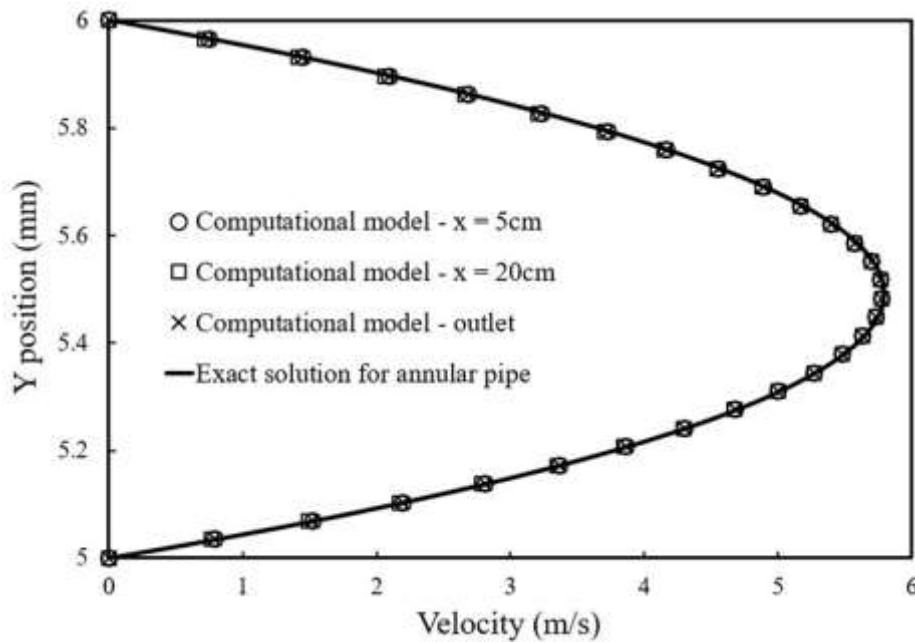


Figure 3. Comparison of predicted velocity profile with the exact solution for fully developed annular flows.

For pipe diffusional deposition of nanoparticles, a dimensionless diffusion parameter  $\sigma_d$  was defined by (Ingham 1976), which is given as,

$$\sigma_d = \frac{\tilde{D}L_{pipe}}{U_{in}d_h^2} \quad (7)$$

Here  $\tilde{D}$  is the diffusivity,  $L_{pipe}$  is the length of the pipe,  $U_{in}$  is the inlet velocity and  $d_h$  is the hydraulic diameter.

In the case of a flat rectangular channel, (Ingham 1976; Kerouanton, Tymen, and Boulaud 1996) developed an asymptotic solution for the deposition efficiency for  $\sigma_d \leq 0.005$  that is,

$$DE = 7.3945\sigma_d^{2/3} + 1.6\sigma_d + 0.803\sigma_d^{4/3} \quad (8)$$

It was shown by Kerouanton et al. (1996) that for  $\sigma_d \leq 0.005$  and when the ratio of inner to the outer diameter of  $d_i/d_o > 0.25$ , the diffusional deposition efficiency for annular pipe is the same as that for a flat rectangular duct developed by Ingham (1976). These analytical approaches were also matched with experimental studies in the literature (Malet et al. 2000).

For evaluating the deposition efficiency in a fully developed flow, at the injection plane at the inlet, the particle flux profile was generated using the velocity given by Eq. (5). Then, the deposition efficiency is calculated based on the ratio of mass deposition rate on the wall to the inlet mass flow rate of particles as (Longest and Xi 2007). That is,

$$DE = \frac{\dot{m}_w}{\dot{m}_{in}} \quad (9)$$

where  $\dot{m}_w$  and  $\dot{m}_{in}$  are, respectively, the mass flux of deposited and injected particles.

For integrating the particle equation of motion, as well as, for evaluating the Brownian force term, the integration time-step size should be selected. The time-step size is defined as the ratio of length scale factor ( $L_s$ ) to the summation of particle and continuous phase velocities. That is,

$$\Delta t = \frac{L_s}{u_p + u_c} \quad (10)$$

where  $L_s$  is an approximate distance that the particle moves in one time step (Inthavong, Tian, and Tu 2016) which is considered 1 micron after assessing different values of the length scale factor. To validate the computational model, in Figure 4 the predicted deposition efficiency of particle in a smooth annulus using the axisymmetric model are compared with the Ingham's equation given by Eq. (8). Here the particles are injected at  $x=5\text{cm}$  in the fully developed region. It is seen that there is a good agreement of the simulated deposition efficiency with the Ingham equation. Note that the value of  $\sigma_d$  is less than 0.005 for the conditions used in this study and therefore the Ingham equation can be used. The favorable comparison in Figure 4 indicates that the axisymmetric flow model in conjunction with the Lagrangian particle tracking approach can be used to evaluate the deposition of nano-particles in annular pipes.

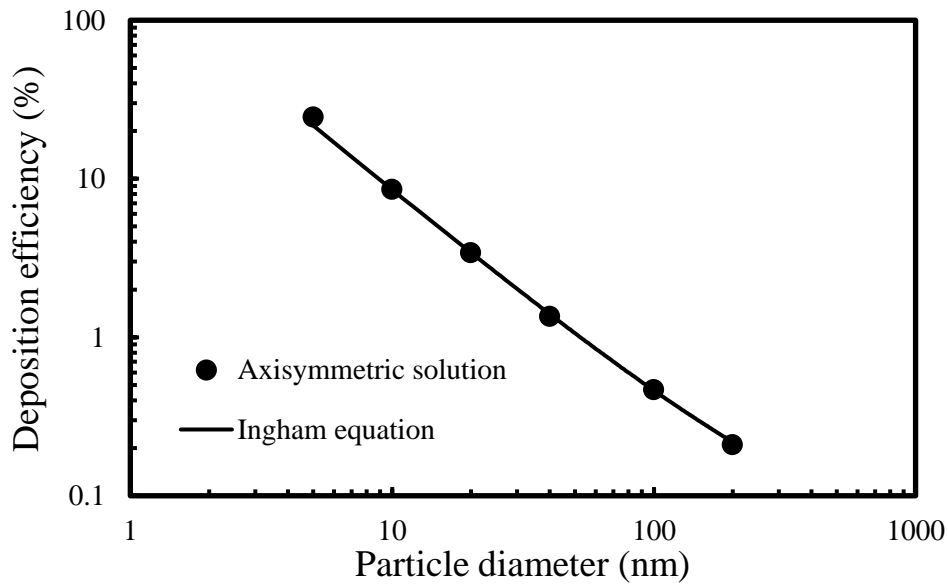


Figure 4. Comparison of the predicted deposition efficiency versus particle diameter with Ingham's equation.

#### 4.2. Flow field and particle deposition analysis

Figures 5 and 6 display, respectively, the velocity contours and the velocity vector fields in the cavities of different studied tread geometries. The formation of recirculating vortices inside the thread cavities is clearly seen from these figures. Inside the thread cavities, the velocity magnitude is small and if a particle enters into the recirculation region, is likely the particle will deposit by the diffusional mechanics, which is large for nanoparticles. In smooth annulus pipes, only the Brownian diffusion contributes to the particle deposition. In annular pipes with threads, however, the generated vertical flow inside the thread cavity caused particle capture by the recirculating flows and enhances the deposition rate.

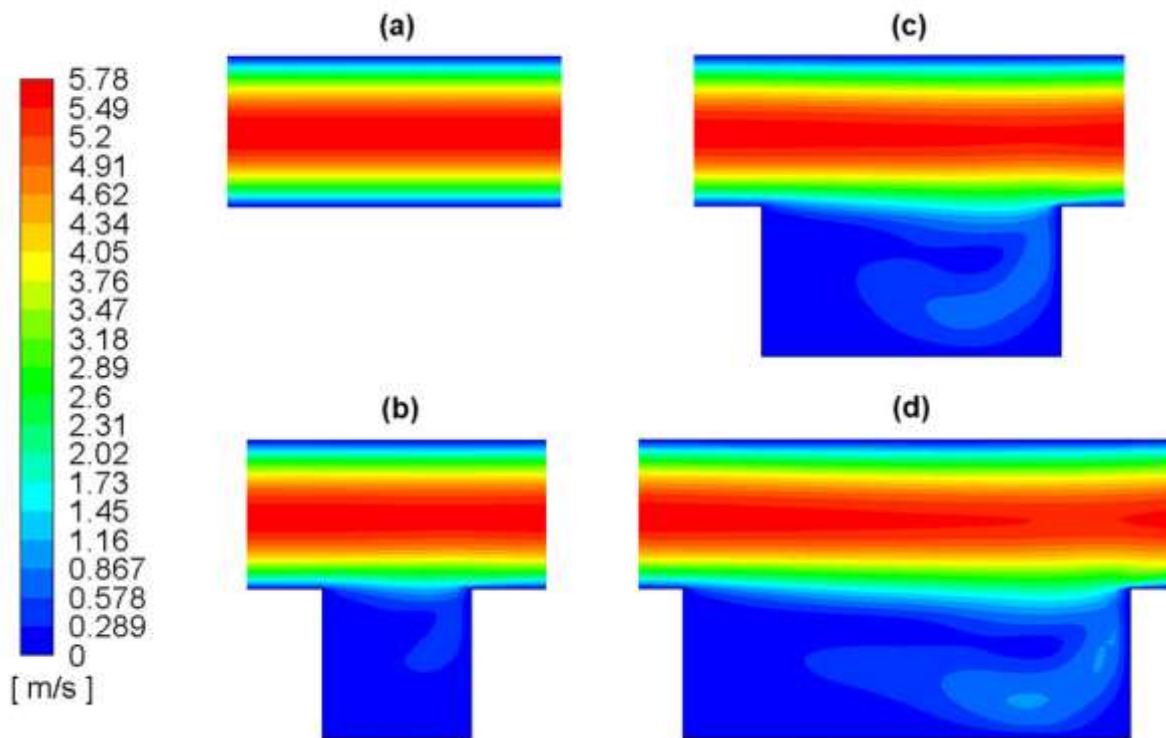


Figure 5. The velocity contours for different studied tread geometries in annular pipes. a)

Smooth pipe. b) 1mmcavity. c) 2mm cavity. d) 3mm cavity..

From Figure 6, it is seen that the recirculation region is stretched as the thread cavity length increases. It is conjectured that for longer thread length, the particle deposition rate increases due to the availability of additional surface area.

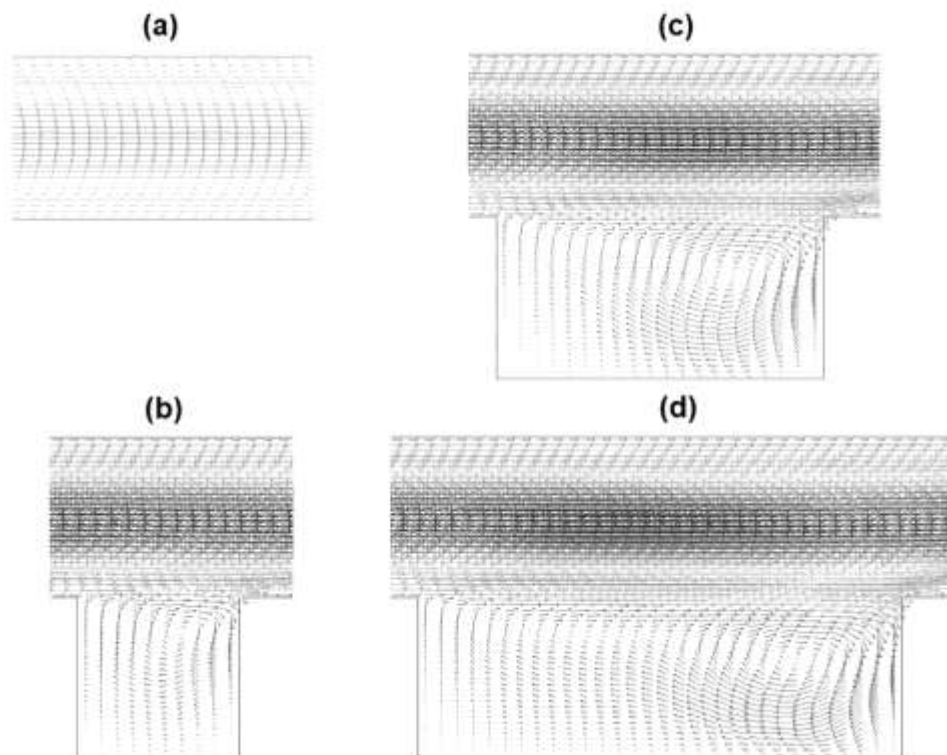


Figure 6. The velocity vectors for different studied tread geometries in annular pipes. a) Smooth pipe. b) 1mm long thread cavity. c) 2mm long thread cavity. d) 3mm long thread cavity.

Figure 7 displays sample trajectories of 5 nm particles inside the annular pipe with two 2mm long threads. In this case, the flow mean velocity is 3.86 m/s and 100 particles were released within the

height of 0.05 mm from the inner surface of the main channel. The figure shows three sample trajectories of the deposited particles by different mechanisms:

- 1- The particles are deposited due to the Brownian diffusion in the main passage outside the thread in the entrance length, between the threads and in the exit length.
- 2- The particles are deposited in the thread cavity due to the effect of Brownian motion, which cause the particle to deviate from the flow streamlines and be captured by the wall. For 5nm particles, the inertia effect is negligible compared to the Brownian diffusion, so the deviation from the streamlines is mainly due to the Brownian motion.
- 3- The particles are captured by the recirculating flow in the thread cavity and after some time, they are deposited on the walls by the Brownian motion.

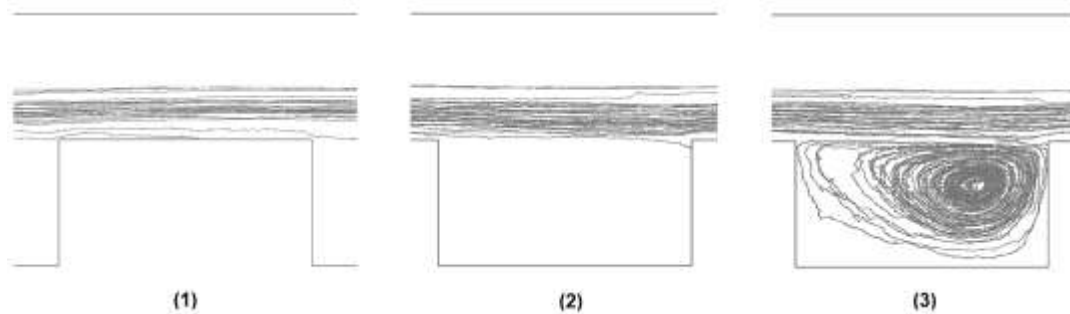


Figure 7. Sample trajectories of deposited 5nm particles in the annulus with 2mm threads.

Figure 8 displays the trajectories of 200nm particles near the thread. Particles were initially released within a distance of 0.05mm from the main channel surface. It is seen that most of the particles that enter the thread cavity are deposited on the wind side wall. It is conjectured that this is due to higher inertia of 200 nm particles compared to the 5 nm particles. In addition, a small fraction of 200nm particles are deposited on the main channel walls due to Brownian diffusion, although the particle diffusion intensity is low. Compared with 5nm particles, the 200nm particles

are rarely captured by the recirculating flow inside the thread cavities due to their high inertia and they typically deposit at the wind side wall inside the thread cavity.

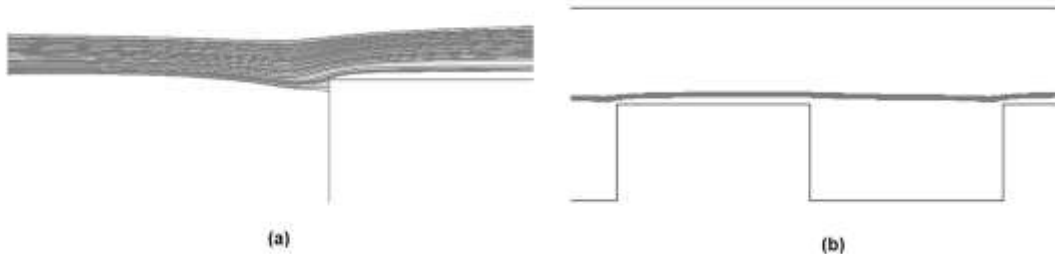


Figure 7. Sample trajectories of deposited 200nm particles in a thread.

Figure 8 illustrates the simulated deposition efficiency when the particles are injected from the inlet. As mentioned before, the deposition efficiency is calculated as the ratio of number of deposited particles to the total number of injected particles. For particle diameters less than 40nm, the deposition efficiency in the annular pipe with and without threads are almost the same. However, for larger particle diameters, the presence of thread increases the deposition efficiency. The reason is that in the threaded cases, the inertia effect becomes more important causes additional deposition. Note that in addition to the near wall particles, particles may deviate from the streamlines due to the Brownian diffusion and get captured into the recirculating flow inside the thread cavities and then deposited. It is also seen that the deposition efficiency of the annuli with 2mm and 3mm threads are roughly the same. Furthermore, the deposition results are the same when the particles are injected at the fully developed region at  $x=5\text{cm}$  and therefore the results are not repeated for the sake of brevity.



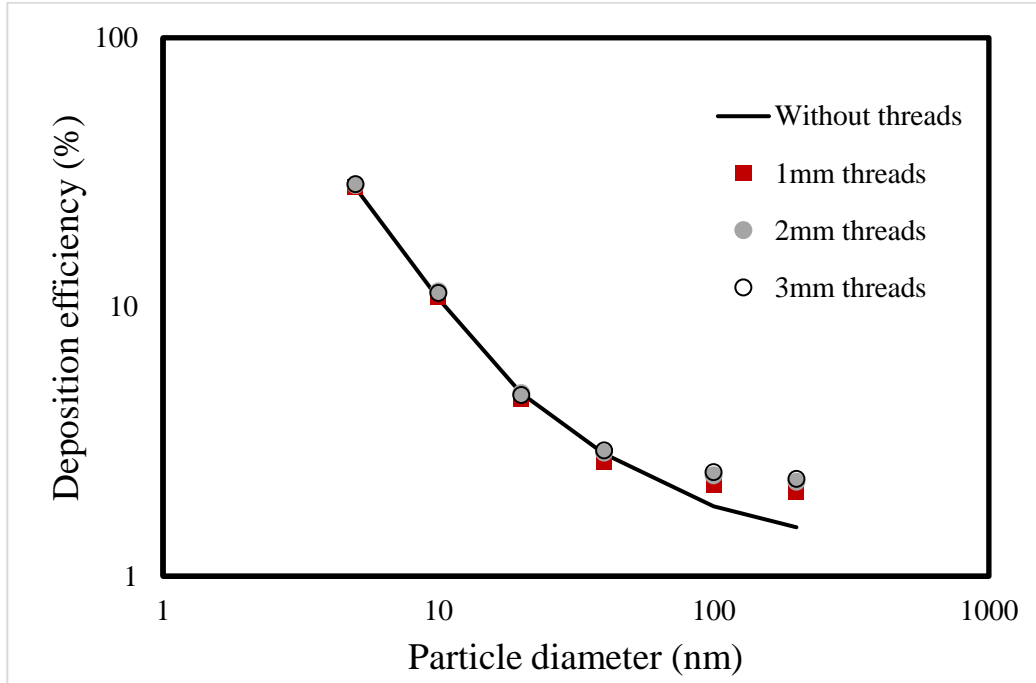


Figure 9. Comparison of deposition efficiencies of nanoparticles released at the inlet for annular pipes with and without threads.

Table 1 presents the deposition efficiencies of nanoparticles in annular pipes with the lengths of 40cm and 60cm for the thread lengths of 2mm. Note that, the lengths of flat entrance and exit section are constant equal to 10cm for both cases. Table 1 shows that by increasing the length of annular pipe, more particles are deposited on the walls. However, the effect of pipe length reduces as the diameter of nanoparticles increases. The reason is due to the increasing effect of Brownian diffusion for smaller nanoparticles.

Table 1. Deposition efficiency of nanoparticles for various lengths of threaded annular pipe

Particle diameter	5nm	10nm	20nm	40nm	100nm	200nm

DE: L=60cm	36.57%	14.67%	5.76%	3.08%	2.51%	2.33%
DE: L=40cm	28.41%	11.44%	4.79%	2.88%	2.37%	2.25%

Figure 10 illustrates the number of deposited particles at different surfaces of the annular pipe for various nanoparticle diameters for a pipe length of 60cm. The surfaces include the upper wall and the flat part of the inner wall in the entrance region, the exit region, the walls between the thread cavities (shown as between threads), the walls inside the thread cavities (shown as inside threads), and the total walls of the inner tube (inner wall). As mentioned before, for the 60cm long threaded annular pipe, the entrance, the threaded area and the exit length are, respectively, 10cm, 40cm and 10cm. For particles less than 40nm, the number of deposited particles on the upper wall are higher than other parts of the annular pipe. However, for larger 200nm nanoparticles, the number of deposited particles inside the threads is higher than the upper wall. An important finding is that as the particle diameter increases, smaller number of particles is deposited on the flat surface between the thread cavities and the exit wall. The number of deposited particles for 100nm and 200nm on the flat surface of the exit wall and between thread cavities are zero and also is also negligible for 40nm particles. The reason is that due to their higher inertia these larger nanoparticles move along the streamlines and do not deviate from them. Therefore, they pass over the walls including those between the thread cavities and do not deposit. Generally the total number of deposited particles on the inner tube is higher than that on the upper tube due to the larger surface area of the inner pipe. This is particularly the case for larger 100nm and 200 nm particles.

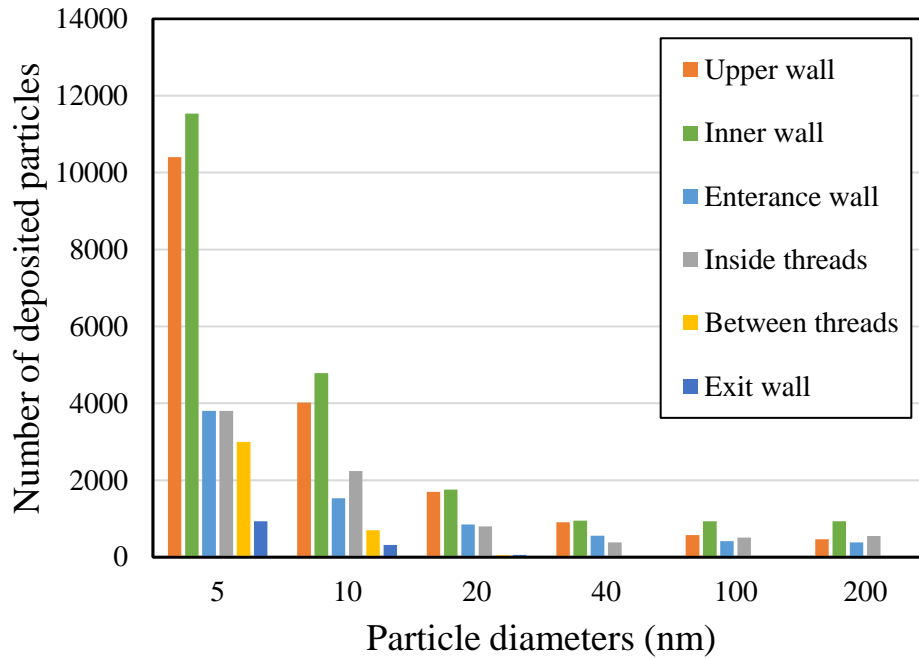


Figure 10. The variation of the number of deposited particles at different surfaces of the annular pipe with a length of 60cm.

## 5. Conclusions

In this paper, the Lagrangian particle tracking method was used and the deposition of nanoparticles in annular pipes with threads was predicted. Different configurations of annular pipes with threads, as well as, a smooth annular pipe were examined. Effects of the tube length and size of nanoparticles were also studied. The computational models for flow velocity and particle deposition efficiency were verified by comparing the results with the analytical solutions and empirical equations reported in the literature. The results showed that an axisymmetric flow model and the Lagrangian particle tracking approach can evaluate the deposition of nano-particles in annular pipe with and without threads. Furthermore, adding threads to the inner surface of the annulus increases the deposition rate of 100 to 200nm particles due to the inertia effect which are

deposited on the flat surface of the exit wall and inside the tread cavities. It can be concluded that for 5 to 200 nm nanoparticles, it was confirmed that the Brownian diffusion was the main deposition mechanism in both treaded and non-threaded annular pipes. The effect of the threads on deposition of smaller nanoparticles was quite small due to their negligible inertia compared to their Brownian diffusion. In other words, for the threaded annulus, for small nanoparticles (less than 40nm), the Brownian diffusion is the dominant mechanism of particle diffusion. For larger particles (more than 100nm), the inertia effect appears to also contribute to particle deposition.

It is noteworthy that this paper provides a numerical investigation on the application of thread addition in nano-particle deposition in a laminar annular pipe flows. The small amount of the collection efficiency is hardly detected in the experimental configuration and real applications; however, this study proves the application of threaded annular pipe which can be used in different applications of nanoparticle technology. The collection efficiency can be improved by increasing the length of the system or optimizing the thread configuration. The results of this study provide insight into the effect of presence of threads on the increasing the capture efficiency of nanoparticles, which may find applications in improving the effectiveness of after treatment systems.

## **References**

Abouali, Omid, and Goodarz Ahmadi. 2005. "A model for supersonic and hypersonic impactors for nanoparticles." *Journal of Nanoparticle Research* 7 (1):75-88. doi: 10.1007/s11051-004-7910-3.

"ANSYS Fluent Theory Guide, ANSYS, Inc." In. 2018.

- Chang, Y. C., M. B. Ranade, and J. W. Gentry. 1995. "Thermophoretic Deposition in Flow along an Annular Cross-section: Experiment and Simulation." *Journal of Aerosol Science* 26 (3):407-28. doi: 10.1016/0021-8502(94)00118-I.
- Chaumeil, Florian, and Martin Crapper. 2014. "Using the DEM-CFD method to predict Brownian particle deposition in a constricted tube." *Particuology* 15:94-106. doi: <https://doi.org/10.1016/j.partic.2013.05.005>.
- Chen, Fangzhi, CM Simon, and Alvin CK Lai. 2006. "Modeling particle distribution and deposition in indoor environments with a new drift-flux model." *Atmospheric Environment* 40 (2):357-67.
- Cohen, B. S., and B. Asgharian. 1990. "Deposition of Ultrafine Particles in the Upper Airways: An Empirical Analysis." *Journal of Aerosol Science* 21 (6):789-97. doi: 10.1016/0021-8502(90)90044-X.
- Ge, Q., K. Inthavong, and J. Tu. 2012. "Local Deposition Fractions of Ultrafine Particles in a Human Nasal-Sinus Cavity CFD Model." *Inhalation Toxicology* 24 (8):492-505. doi: 10.3109/08958378.2012.694494.
- Goula, Athanasia M, Margaritis Kostoglou, Thodoris D Karapantsios, and Anastasios I Zouboulis. 2008. "A CFD methodology for the design of sedimentation tanks in potable water treatment: Case study: The influence of a feed flow control baffle." *Chemical Engineering Journal* 140 (1):110-21.
- He, Chunhong, and Goodarz Ahmadi. 1999. "Particle deposition in a nearly developed turbulent duct flow with electrophoresis." *Journal of Aerosol Science* 30 (6):739-58. doi: 10.1016/S0021-8502(98)00760-5.

- Ingham, D. B. 1975. "Diffusion of aerosols from a stream flowing through a cylindrical tube." *Journal of Aerosol Science* 6 (2):125-32. doi: 10.1016/0021-8502(75)90005-1.
- . 1976. "Simultaneous diffusion and sedimentation of aerosol particles in rectangular tubes." *Journal of Aerosol Science* 7 (5):373-80. doi: 10.1016/0021-8502(76)90023-9.
- . 1991. "Diffusion of aerosols in the entrance region of a smooth cylindrical pipe." *Journal of Aerosol Science* 22 (3):253-7. doi: 10.1016/S0021-8502(05)80003-5.
- Inthavong, Kiao, Lin Tian, and Jiyuan Tu. 2016. "Lagrangian particle modelling of spherical nanoparticle dispersion and deposition in confined flows." *Journal of Aerosol Science* 96:56-68. doi: <https://doi.org/10.1016/j.jaerosci.2016.02.010>.
- Inthavong, Kiao, Kai Zhang, and Jiyuan Tu. 2009. "Modeling Submicron and Micron Particle Deposition in a Human Nasal Cavity." In *Seventh International Conference on CFD in the Minerals and Process Industries*. Melbourne, Australia: CSIRO.
- Jayarathne, ER, C He, ZD Ristovski, L Morawska, and GR Johnson. 2008. "A comparative investigation of ultrafine particle number and mass emissions from a fleet of on-road diesel and CNG buses." *Environmental science & technology* 42 (17):6736-42.
- Johnson, Timothy V. 2009. "Diesel emission control in review." *SAE international journal of fuels and lubricants* 1 (1):68-81.
- Kennedy, Ian M. 2007. "The health effects of combustion-generated aerosols." *Proceedings of the Combustion Institute* 31 (2):2757-70. doi: <https://doi.org/10.1016/j.proci.2006.08.116>.
- Kerouanton, D., G. Tymen, and D. Boulaud. 1996. "Small Particle Diffusion Penetration of an Annular Duct Compared to other Geometries." *Journal of Aerosol Science* 27 (2):345-9. doi: 10.1016/0021-8502(95)00561-7.

- Kittelson, David B. 1998. "Engines and nanoparticles: a review." *Journal of Aerosol Science* 29 (5):575-88. doi: [https://doi.org/10.1016/S0021-8502\(97\)10037-4](https://doi.org/10.1016/S0021-8502(97)10037-4).
- Kwak, JH, HS Kim, JH Lee, and SH Lee. 2014. "On-road chasing measurement of exhaust particle emissions from diesel, CNG, LPG, and DME-fueled vehicles using a mobile emission laboratory." *International Journal of Automotive Technology* 15 (4):543-51.
- Lamb, H., and R. Caflisch. 1993. *Hydrodynamics*: Cambridge University Press.
- Li, A., and G. Ahmadi. 1992a. "Dispersion and Deposition of Spherical Particles from Point Sources in a Turbulent Channel Flow." *Aerosol Science Technology* 16:209-26. doi: 10.1080/02786829208959550.
- . 1992b. "Dispersion and deposition of spherical particles from point sources in a turbulent channel flow." *Aerosol Science and Technology* 16:209-26. doi: 10.1080/02786829208959550.
- . 1993. "Computer simulation of deposition of aerosols in a turbulent channel flow with rough wall." *Aerosol Science Technology* 18:11-24. doi: 10.1080/02786829308959581.
- Lin, Jian-Zhong, Zhao-Qin Yin, Pei-Feng Lin, Mning-Zhou Yu, and Xiao-Ke Ku. 2015. "Distribution and penetration efficiency of nanoparticles between 8–550 nm in pipe bends under laminar and turbulent flow conditions." *International Journal of Heat and Mass Transfer* 85:61-70.
- Lin, Jianzhong, Peifeng Lin, and Huajun Chen. 2009. "Research on the transport and deposition of nanoparticles in a rotating curved pipe." *Physics of fluids* 21 (12):122001.
- Lin, Jianzhong, Zhaoqin Yin, Fujun Gan, and Mingzhou Yu. 2014. "Penetration efficiency and distribution of aerosol particles in turbulent pipe flow undergoing coagulation and breakage." *International Journal of Multiphase Flow* 61:28-36.

- Longest, P. Worth, and Jinxiang Xi. 2007. "Effectiveness of Direct Lagrangian Tracking Models for Simulating Nanoparticle Deposition in the Upper Airways." *Aerosol Science and Technology* 41 (4):380-97. doi: 10.1080/02786820701203223.
- Malet, J, N Michielsen, D Boulaud, and A Renoux. 2000. "Mass transfer of diffusive species with nonconstant in-flight formation and removal in laminar tube flow. Application to unattached short-lived radon daughters." *Aerosol Science & Technology* 32 (3):168-83.
- Martonen, Ted, Zongqin Zhang, and Yadong Yang. 1996. "Particle Diffusion with Entrance Effects in a Smooth-walled Cylinder." *Journal of Aerosol Science* 27 (1):139-50. doi: 10.1016/0021-8502(95)00530-7.
- Ounis, H., G. Ahmadi, and J. B. McLaughlin. 1993. "Brownian particles deposition in a directly simulated turbulent channel flow." *Physics of Fluids A* 5:1427-32. doi: 10.1063/1.858578.
- Paul, Bireswar, Amitava Datta, Aparna Datta, and Abhijit Saha. 2013. "Optical characterization of nano-sized organic carbon particles emitted from a small gasoline engine." *Particuology* 11 (3):249-55. doi: <https://doi.org/10.1016/j.partic.2012.06.011>.
- Ristovski, Zoran, Lidia Morawska, Godwin A Ayoko, G Johnson, Dale Gilbert, and Chris Greenaway. 2004. "Emissions from a vehicle fitted to operate on either petrol or compressed natural gas." *Science of the Total Environment* 323 (1-3):179-94.
- Sardari, Pouyan Talebizadeh, Hassan Rahimzadeh, Goodarz Ahmadi, and Donald Giddings. 2018. "Nano-particle Deposition in the Presence of Electric Field." *Journal of Aerosol Science* 126:169-79.
- Talebizadeh, P, H Rahimzadeh, G Ahmadi, R Brown, and K Inthavong. 2016a. "Time history of diesel particle deposition in cylindrical dielectric barrier discharge reactors." *Journal of Nanoparticle Research* 12 (18):1-13.



- Talebizadeh, P., H. Rahimzadeh, G. Ahmadi, R. Brown, and K. Inthavong. 2016b. "Time history of diesel particle deposition in cylindrical dielectric barrier discharge reactors." *Journal of Nanoparticle Research* 18 (12):378.
- Talebizadeh, Pouyan, Meisam Babaie, R Brown, Hassan Rahimzadeh, Zoran Ristovski, and M Arai. 2014. "The role of non-thermal plasma technique in NO x treatment: A review." *Renewable and Sustainable Energy Reviews* 40:886-901.
- Talebizadeh, Pouyan, Hassan Rahimzadeh, Meisam Babaie, Saeed Javadi Anaghizi, Hamidreza Ghomi, Goodarz Ahmadi, and Richard Brown. 2015. "Evaluation of residence time on nitrogen oxides removal in non-thermal plasma reactor." *PloS one* 10 (10):e0140897.
- Thomas, J. W. 1967. Assessment of airborne radioactivity.
- Tian, Lin, Yidan Shang, Jingliang Dong, Kiao Inthavong, and Jiyuan Tu. 2017. "Human nasal olfactory deposition of inhaled nanoparticles at low to moderate breathing rate." *Journal of Aerosol Science* 113:189-200.
- Tsai, Chuen-Jinn, Jyh-Shyan Lin, Shankar G. Aggarwal, and Da-Ren Chen. 2004. "Thermophoretic Deposition of Particles in Laminar and Turbulent Tube Flows." *Aerosol Science and Technology* 38 (2):131-9. doi: 10.1080/02786820490251358.
- Wang, SM, K Inthavong, J Wen, JY Tu, and CL Xue. 2009. "Comparison of micron-and nanoparticle deposition patterns in a realistic human nasal cavity." *Respiratory physiology & neurobiology* 166 (3):142-51.
- Wichmann, H. E. 2007. "Diesel Exhaust Particles." *Inhalation Toxicology* 19 (sup1):241-4. doi: 10.1080/08958370701498075.

- Xinling, Li, and Huang Zhen. 2009. "Emission reduction potential of using gas-to-liquid and dimethyl ether fuels on a turbocharged diesel engine." *Science of the Total Environment* 407 (7):2234-44.
- Yeh, H. C., and G. M. Schum. 1980. "Models of human lung airways and their application to inhaled particle deposition." *Bull Math Biol* 42:461-80. doi: 10.1016/S0092-8240(80)80060-7.
- Zamankhan, Parsa, Goodarz Ahmadi, Zuo Cheng Wang, Philip K. Hopke, Yung-Sung Cheng, Wei Chung Su, and Douglas Leonard. 2006. "Airflow and Deposition of Nano-Particles in a Human Nasal Cavity." *Aerosol Science and Technology* 40 (6):463-76. doi: 10.1080/02786820600660903.